

Strain-Life Fatigue Predictions for Sintered Steels with Nonzero Mean Stress

Ernani S. Palma and Paulo C. Greco, Jr.

(Submitted 28 December 1998; in revised form 7 September 2000)

Several approximate models have been utilized for fatigue life prediction. Some of these models are available for mean stress (or strain) correction on fatigue life, when nonzero mean stress (or strain) is applied. In this paper, the most commonly used empirical strain-life models for fatigue life predictions, for materials subjected to variable amplitude loads, are described. Experimental results of fatigue tests, where the specimens of sintered steels were subjected to partial random loads, are presented and compared with those results obtained theoretically by the models. The utilization of the various models and their influence on results are discussed.

Keywords cyclic loads, fatigue, fatigue life prediction, sintered materials, strain life

1. Introduction

Over the past years, considerable effort has been directed at the development and application of quantitative models to estimate the fatigue life of components. Many empirical relationships were developed and they are widely used for material optimization studies.[1–5] Nowadays, a renewed interest on these approximate empirical strain-life prediction models for sintered materials has been observed.[6,7,8] Fatigue properties are becoming important in the application of powder metallurgy (P/M) products. These materials are increasingly used in components subjected to cyclic loads, and performance limitations associated with fatigue failure have arised.[6,8,9] The market demand for P/M materials could increase considerably if problems of fatigue in these materials were solved. As a result, much research effort on fatigue of sintered materials has been carried out and significant advances have been made toward understanding the fatigue behavior of these materials.[6–14] It is well established that the fatigue endurance limit of sintered materials decreases by increasing porosity and by decreasing the roundness of the pores.

Although these efforts are of great importance, they still cannot give a basis for a consistent use of P/M materials where highly reliable components are required and fatigue is known to be a major problem. To date, P/M fatigue properties for use in design are still very limited. Moreover, most service applications involve nonzero mean cyclic stress and nonzero strain, and relatively little attention has been paid to the behavior of porous materials in these situations. Therefore, the purpose of this study is to compare some fatigue life prediction models existing in the literature with experimentally obtained fatigue lifes, when a specimen is subjected to partial random fatigue loads with nonzero mean stress.

Ernani S. Palma and **Paulo C. Greco, Jr.,** Department of Mechanical Engineering, Catholic University of Minas Gerais - PUC.Minas, Belo Horizonte - MG - Brazil. Contact e-mail: palma@pucminas.br.

1.1 Fatigue Life Prediction Models

The strain-life method is based on the conventional strain-life relationship:[15–18]

$$\frac{\Delta\varepsilon}{2} = \frac{\sigma_f'}{E}(2N_f)^b + \varepsilon_f'(2N_f)^c \qquad \text{(Eq 1)}$$

where

$\Delta\varepsilon$ = the total strain range,
σ = the fatigue strength coefficient,
E = the cyclic elastic modulus,
b = the fatigue strength exponent,
ε = the fatigue ductility coefficient,
c = the fatigue ductility exponent, and
$2N_F$ = the number of reversals to failure.

The first term of Eq 1 represents the elastic strain component, and the second, the plastic strain component. Knowing the four empirical constants (b, c, ε_f', and ε_f'), the strain-life relationship can be evaluated and then used to predict the life of the component.

The cyclic stress-strain curve can be fitted using a power-law hardening model, and consequently, the total strain can be expressed in another form:[15,17]

$$\varepsilon = \frac{\sigma}{E} + \left(\frac{\sigma}{K'}\right)^{1/n'} \qquad \text{(Eq 2)}$$

where K' is the cyclic strength coefficient and n' is the cyclic strain hardening exponent.

All above-defined fatigue constants can be determined experimentally through linearization of appropriate relationships on log-log coordinates. The consistency of these fatigue empirical constants can be checked by using the relations[15,16]

$$K' = \frac{\sigma_f'}{(\varepsilon_f')^{n'}} \qquad \text{(Eq 3)}$$

and

$$n' = \frac{b}{c} \qquad \text{(Eq 4)}$$

A certain percentage error (up to 20%) between the experimentaly determined properties and those calculated by the above equations (n' and K') is tolerable.[16] Errors over 20% tend to show inconsistency of the data. Most discrepancies in these values arise from inaccurate regression or data analysis.[16]

The cyclic fatigue properties are obtained for completely reversed loads. The majority of engineering components are usually subjected to variable amplitude loads with nonzero mean stress ($\sigma_m \neq 0$). Modifications of Eq 1 have been proposed to take into account the effect of mean stresses distinct from zero. Morrow proposed that only the elastic component of Eq 1 should be influenced by the mean stress σ_m,[15,17,18] that is,

$$\frac{\Delta\varepsilon}{2} = \frac{\sigma_f' - \sigma_m}{E}(2N_f)^b + \varepsilon_f'(2N_f)_c \qquad \text{(Eq 5)}$$

Manson and Halford have considered that both components of Eq 1 are influenced by the presence of the nonzero mean stress. Thus, the final correlation between total strain amplitude and fatigue life becomes[15,17]

$$\frac{\Delta\varepsilon}{2} = \frac{\sigma_f' - \sigma_m}{E}(2N_f)^b + \left(\frac{\sigma_f' - \sigma_m}{\sigma_f'}\right)^{c/b} \varepsilon_f'\,(2N_f)^c \qquad \text{(Eq 6)}$$

To characterize the fatigue life behavior, Smith, Watson, and Topper (SWT) have proposed the following equation, which accounts for the mean stress by considering the maximum stress $\sigma_{\max}$:[15,19]

$$\sigma_{\max}\frac{\Delta\varepsilon}{2} = \frac{(\sigma_f')^2}{E}(2N_f)^{2b} + \sigma_f'\varepsilon_f'\,(2N_f)^{b+c} \qquad \text{(Eq 7)}$$

All previous models were derived from Eq 1. Still another empirical model has been proposed to take into account the effect of nonzero mean strain induced by cyclic loads, that is,[20]

$$\Delta\varepsilon = \frac{2(1 - R)\varepsilon_f'}{[(4N_f) - 1)(1 - R)^a + (2)^a]^{1/a}} \qquad \text{(Eq 8)}$$

where $\Delta\varepsilon = \varepsilon_{\max} - \varepsilon_{\min}$, $R = \varepsilon_{\min}/\varepsilon_{\max}$, and $a = -1/c$.

2. Experimental Procedure

2.1 Materials

The raw materials used in this investigation were a Fe-1.78% Cu-0.50% C alloy, made from elemental powders. Samples were made by mixing the powder with 0.5 wt.% lubricant (zinc stearate).

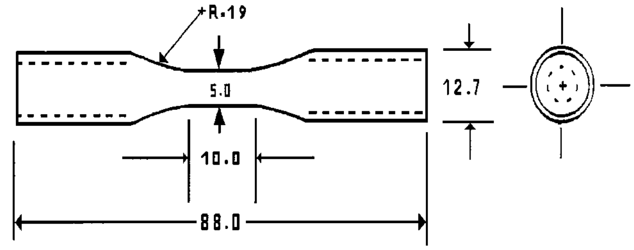

Fig. 1 Fatigue specimens—dimensions in millimeters

Fatigue and tensile specimens with gauge length of 10 mm, as shown in Fig. 1, were produced using a floating die tool. The applied compacting pressure was such that two levels of as-sintered porosities $P_0 = 10.8 \pm 0.7\%$ and $5.6 \pm 0.3\%$ (here, designated FCA and FCB, respectively) were produced. The specimen sinterization was carried out for 40 min at 1150 °C in a 80% nitrogen-20% hydrogen atmosphere. Finish grinding was carried out to achieve a surface finish $R_A = 2.1 \pm 0.3$ μm in the gauge length.

2.2 Apparatus and Conditions

Experimental fatigue tests were carried out on a closed-loop servohydraulics testing machine, with stress and strain control at room temperature. The stress and strain values were obtained by simultaneously recording measurements of applied load with a load cell and the applied strain with an extensometer.

In the stress- and strain-controlled tests, each specimen was subjected to cyclic load until either the specimen failed or achieved two million cycles, which was considered a run-out criterium. All these tests were performed with zero mean stress and zero mean strain ($R = -1$), and with frequency equal to 5 Hz. Approximately 11 to 20 specimens from each porosity were used to obtain the stress life and strain life. Cyclic stress-strain curves were obtained by testing several specimens at various strain levels. Since the hysteresis loops did not have the tendency to stabilize, the fatigue properties were determined at half-life ($N_F/2$), that is, the stress and strain values for approximately 50% of the total fatigue life were recorded.

In addition, 11 specimens of each porosity were subjected to partially random uniaxial tensile load, as shown in Fig. 2. Compression loads were not used to avoid bending. Each load block was repeated time after time until failure took place. In order to compare specimens with distinct mechanical properties, a maximum tensile load corresponding to 80% of yield strength of each porosity was applied.

Uniaxial tensile tests (monotonic) were perfomed on the same test machine used in the fatigue tests. The values of stress and strain were automatically recorded by a PC. Four specimens of each porosity were tested to ensure repeatability.

3. Results

All the fatigue data for these materials are summarized in Table 1. The fatigue parameters of the wrought (pore-free)

Table 1 **Fatigue parameters of materials**

Material	Porosity (%)	E (GPa)	K' (MPa)	n'	σ'_f (MPa)	ε'_f	b	c	Ref.
FCA	10.8	117.2	887.2	0.208	774.5	0.178	−0.156	−0.819	···
FCB	5.6	168.4	1042.3	0.163	891	0.316	−0.122	−0.730	···
1045	0	207	2636	0.120	2165	0.220	−0.080	−0.660	16

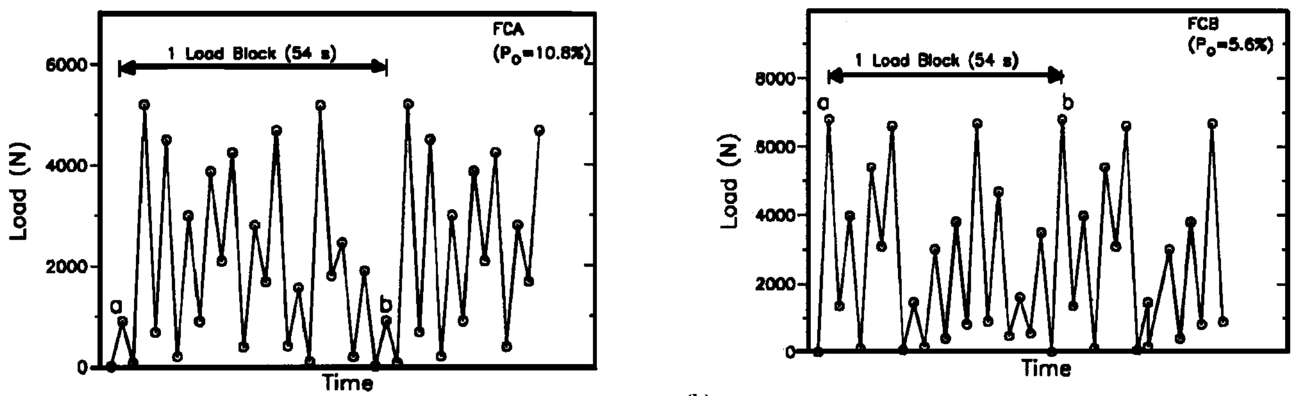

(a) (b)

Fig. 2 Load sequences: (**a**) FCA—P_0 = 10.8%; and (**b**) FCB—P_0 = 5.6%

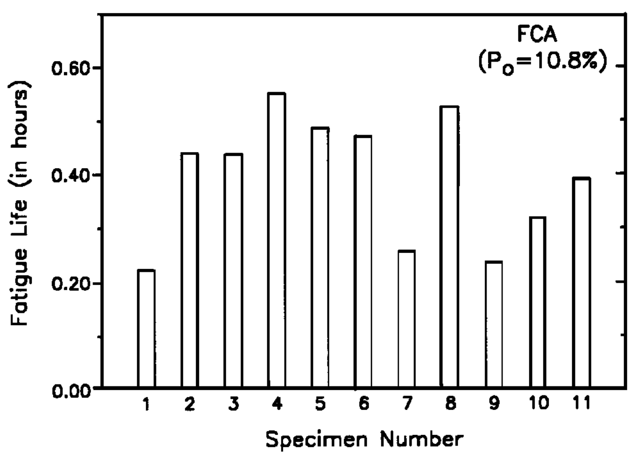

Fig. 3 Experimental fatigue life for FCA, subject to partial random loads

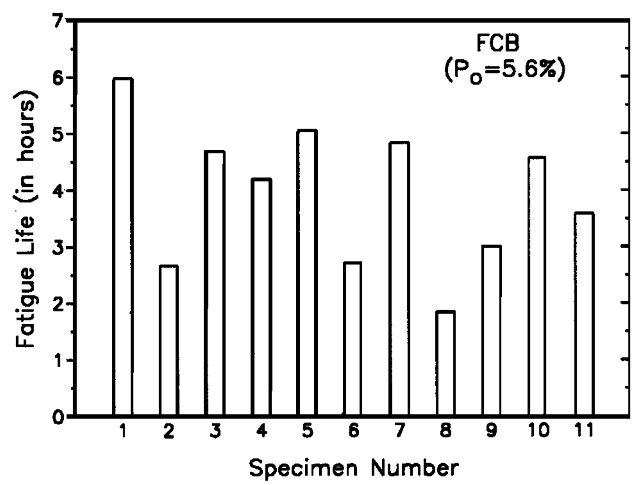

Fig. 4 Experimental fatigue life for FCB, subject to partial random loads

AISI-1045 steel, with Brinell hardness equal to 500 BHN, are also shown in Table 1. This steel was chosen because it is used in machine components and will be used as a reference.[16]

Eleven specimens of FCA and FCB were subjected to axial loading that fluctuates, as shown in Fig. 2, where each load block had a duration of 54-s. This load block was repeated until the specimen failed, and the life was recorded (in h). The results of these experiments are shown in Fig. 3 and 4 for FCA and FCB, respectively.

In order to perform theoretical fatigue life prediction for FCA and FCB materials, the stress values were related to the experimental loads (Fig. 2) through the cross-sectional area of the specimens. The rain flow cycle counting method was employed to determine the maximum and minimum values of each stress reversal in the typical 54-s block of loading. From these stress peaks, corresponding values of maximum and minimum strain were determined by using Eq 2.

$$\varepsilon = \frac{\sigma}{E} + \left(\frac{\sigma}{K'}\right)^{1/n'} \qquad \text{(Eq 9)}$$

The theoretical failure lifes in cycles (N_F), associated with each level within of the 54-s loading block, were determined by using

Table 2 Theoretical time necessary to failure

Model	Theoretical fatigue life (h)	
	FCA	FCB
Conventional—Eq 1	4.02	118.88
Morrow—Eq 5	2.35	44.77
Manson—Eq 6	1.23	20.66
SWT—Eq 7	3.19	37.96
Ohji—Eq 8	0.57	5.19

Table 3 Consistency of fatigue empirical parameters

Property		FCA	FCB	AISI 1045
K' (MPa)	Experimental	887	1042	2636
	Eq 3	978	1033	2596
	Error (%)	10.3	1	1.5
n'	Experimental	0.208	0.163	0.120
	Eq 4	0.190	0.167	0.121
	Error (%)	8.7	2.5	0.8

all the above-described models, through an iterative numerical process. All required parameters were previously determined with the exception of $a = -1/c$ for Eq 8. Then, utilizing the Miner linear damage rule, the damage (D) associated with each 54-s loading block can be determined, $D = (1/N_F)$. Finally, the time (t) necessary to reach total damage, or theoretical fatigue life, can be estimated by using

$$\frac{t_c}{54} \sum\left(\frac{1}{N_F}\right) = 1 \qquad \text{(Eq 10)}$$

the values of which are shown in Table 2.

4. Discussion

The fatigue data consistency was checked by using Eq 3 and 4, and the results are shown in Table 3. All properties of FCA, FCB, and 1045 show very good self-consistency, since the difference between experimental and calculated data is relatively small, with errors less than 10.3%. For P/M materials, these errors increase with increasing porosity. The cyclic strength coefficients K' increase with decreasing porosity, while the cyclic strain hardening exponents n' decrease with decreasing porosity. If the pore-free 1045 steel and the sintered material FCB are compared, the errors in both parameters are similar.

As expected, all models predict shorter lifes for FCA ($P_0 = 10.8\%$) than for FCB ($P_0 = 5.6\%$), due to the difference in porosity. These models can be divided in three groups. The first group includes only the conventional model, Eq 1, which does not consider the influence of mean stress. Thus, the obtained lives are too large in comparison with other models. The second group includes the Morrow, Manson, and SWT models, which were derived from the conventional strain-life equation to account for mean stress effects. In general, the theoretical fatigue lives predicted by the models in this group are similar. The Morrow model, by considering influence of mean stress only on the elastic term, incorrectly predicts that the ratio of elastic to plastic strain is dependent on mean stress. Consequently, this model should give larger lives than the other models of this group. However, surprisingly, the Morrow model predicted a shorter life for FCA than did the SWT model. The mean stress correction in the SWT model is done by assuming that the controlling factor is the product of the maximum stress and strain amplitude. Thus, because the SWT model considers the influence of mean stress by using the strain amplitude, it was expected that this model should be more conservative than the Manson model, which was confirmed in Table 2 for both sintered materials. Finally, the model proposed by Ohji constitutes the third group, and it is the least conservative, giving the shortest predicted lives. Unlike the other groups, this model takes into account the mean strain (and not mean stress) induced by the external loading. Since the applied loads are relatively large, until approximately 80% of yield stress of each material, the process seems to be dominated by plastic strain. This fact becomes more important due to the presence of pores, which lead to an inhomogenous deformation on microscopic scale.

By comparing Fig. 3 and 4 with Table 2, it can be observed that the experimental fatigue lives are shorter than the model predictions, even if the Ohji model is used. This is the unique model that had the tendency to give approximate results. However, due to the porosity in sintered materials, and consequently the pore notch effect, the local strain in the pore vicinity is quite larger than that calculated by the model. This discrepancy becomes more significant if residual stresses are considered. Due to pore notch effect, the loading history leads to tensile overload, which causes the material at the root of the notch (pore) to yield in tension. When the load is released, this material will be in residual compression. Appropriate corrections, which take into account these stress concentration effects of pores and their interations, have to be done to improve the fatigue life prediction.

5. Conclusions

In light of the results and discussions presented above, the following conclusions can be drawn.

- The consistency of empirical fatigue parameters of sintered materials are very good. The errors of FCB material are similar to those of pore-free AISI-1045 steel.
- The models can be divided into three groups, each one with quite different results. The results are relatively similar within each group.
- All analyzed models predicted shorter fatigue lifes for FCA than for FCB sintered steels, due to the higher porosity percentage of FCA.
- Neither model was able to properly predict the experimental fatigue lifes, which are shorter than those theoretically

obtained. Only the Ohji model gave results, which are close to those obtained by experimental tests.

- Corrections have to be made on the Ohji model, to take into account the porosity notch effects.

References

1. W. Schütz: *Proc. 4th Int. Conf. on Structural Failure, Product Liability and Technical Insurance*, H.P. Rossmanith, Vienna, Austria, 1993, vol. 4, p. 49-60.
2. T. Goswani: *Int. J. Fatigue*, 1997, vol. 19 (2), pp. 109-15.
3. P.J. Laz and B.M. Hillberry: *Int. J. Fatigue*, 1998, vol. 20 (4), pp. 263-70.
4. D.L. Duquesnay, M.A. Pompetzki, and T.H. Topper: "Fatigue Life Prediction for Variable Amplitude Strain Histories," Paper no. 930400 of SAE SP-1009 Report—Fatigue Research and Applications, Nov. 1993, pp. 75-185.
5. A. Fatemi and L. Yang: *Int. J. Fatigue*, 1998, vol. 20, pp. 9-34.
6. S.A. Hudson, J.J. Fulmer, and D.R. Griffith: "Characterization of a High Performance P/M Steel for Use in Fatigue Design," Paper no. 930408 of SAE SP-1009 Report—Fatigue Research and Applications, Nov. 1993, pp. 237-45.
7. C.M. Sonsino: *Powder Metall.*, 1990, vol. 33 (3), pp. 235-45.
8. K.D. Christian and R.M. German: *Int. J. Powder Metall.*, 1995, vol. 31 (1), pp. 51-60.
9. G. Straffelini, V. Fontanari, A. Molinari, and B. Tesi: *Powder Metall.*, 1993, vol. 36(2), pp. 135-41.
10. E. Klar, D.F. Berry, P.K. Samal, J.J. Lewandowski, and J.D. Rineyetall: *Int. J. Powder Metall.*, 1995, vol. 31 (4), pp. 317-24.
11. J. Holmes and R.A. Queeney: *Powder Metall.*, 1985, vol. 28 (4), pp. 231-35.
12. F.J. Esper, G. Leuze, and C.M. Sonsino: *Powder Metall. Int.*, 1981, vol. 13 (4), pp. 203-08.
13. B. Kubicki: *Sintered Machine Elements*, Ellis Horwood, New York, NY, 1995.
14. B. Kubicki: *Powder Metall.*, 1995, vol. 38 (4), pp. 295-98.
15. J.A. Bannantine, J.J. Comer, and L.L. Handrock: *Fundamentals of Metal Fatigue Analysis*, Prentice-Hall, Englewood Cliffs, NJ, 1990.
16. F.P. Brenna: *Int. J. Fatigue*, 1994, vol. 16, pp. 351-56.
17. E. Zahavi: *Fatigue Design—Life Expectancy of Machine Parts*, CRC Press, Inc., New York, NY, 1996.
18. A. Tricoteaux, F. Fardoun, S. Degallaix, and F. Sauvage: *Fatigue Fract. Eng. Struct.*, 1995, vol. 18 (2), pp. 189-200.
19. K.N. Smith, P. Watson, and T.H. Topper: *J. Mater.*, 1970, vol. 5 (4), pp. 767-78.
20. J.A. Collins: *Failure of Materials in Mechanical Design*, 2nd ed., John Wiley & Sons, New York, NY, 1981, pp. 401-04.